Relative velocity between particle and fluid in a two-phase turbulent flow

Vai Kuong Sin
Faculty of Science and Technology, University of Macau
P. O. Box 3001, Macao SAR, China

Abstract: - A numerical study is presented for relative velocity between particle and fluid in a grid-generated turbulent flow field which is simulated by a two-equation turbulence (k-ϵ) model. Spatial behavior of this velocity is important in the determination of particle dispersion. Both linear and nonlinear drag formulations are considered in detail. Numerical results show that, for nonlinear drag formulation, the occurrence of the maximum value of relative velocity is well ahead of the location where the particle dispersion measurement is taken in the experiment. Hence, better predictions of particle dispersion obtained with the nonlinear drag formulation should be expected. it is also found that the mean square relative velocity components in the gravity direction and in the direction normal to the gravity reach the maximum values at different times.

Key-Words: - Computational fluid dynamics, Mean square relative velocity, Turbulence, Two-phase flow.

1 Introduction

Particle dispersion in turbulent flow can be found in many industrial processes and in nature. Relevant examples from industry are settling and flocculation of "red muds" in the aluminum extraction, pneumatic transport of particles, and combustion of liquid and pulverized solid fuels. In nature, convective transport and settling of particulate phase in the atmosphere, in oceans or in rivers are of extreme importance in the analyses of environmental impact. For the most part, attention had been focused in the past on the dispersion of particles and the settling velocity of particles by turbulence. In the prediction of these properties, it is important that the predicted results are free from the effect of the initial conditions at which the particles are injected into the turbulent flow field. One way to verify this condition is to calculate the temporal behaviour of the relative velocity between particle and fluid, and to find out the maximum value of the relative velocity[1]. The mean square relative velocity between the particle and the fluid, $\overline{u_{i,rel}^2(t)}$, is defined as

$$\overline{u_{i,rel}^2(t)} = \overline{(u_{pi}(t) - u_i(t))^2} \qquad (1)$$

where $u_{pi}(t)$ and $u_i(t)$ are velocities of particle and fluid, respectively, and the overbar denotes ensemble average. Mean square relative velocity was studied by Yeh and Lei[2] with large eddy simulation (LES). Later, Elghobashi and Truesdell[3] performed particle dispersion in a decaying isotropic turbulence simulated with direct numerical simulation (DNS). Elghobashi and Truesdell[3]'s result also includes calculation of mean square relative velocity. This important property in turbulent two-phase flow, however, has not been studied in the situation where the turbulent flow field is simulated with the Reynolds-averaged Navier-Stokes (RANS) equation, even though RANS is still one of the most popular methods to simulate turbulence in Computational Fluid Dynamics (CFD) application. In view of this, the paper presents a detailed studies of mean square relative velocity between the particle and the fluid in a turbulent flow field which is simulated by using Reynolds-averaged Navier-Stokes (RANS) equations with the k-ϵ model. Experimental data of Snyder & Lumley[4] is used for comparison purpose. The grid-generated turbulent flow field used in the experiment[4] is emulated numerically. For this purpose a general CFD code[5] is used, along with a low Reynolds number k-ϵ model to take into account the effect of turbulence upon the mean flow field. The code adopts a finite volume technique to integrate the transport equations written in a generalized coordinate system. The SIMPLEC algorithm is employed to couple the momentum and the continuity equations.

2 Turbulence simulation using two-equation k-ϵ model

The grid-generated steady-state turbulent flow field of Snyder and Lumley[4] is simulated by a general CFD code[5], which solves the 3-dimensional Navier-Stokes equations for a generic mean Cartesian velocity component U_i given in tensor notation as

Continuity equation

$$\frac{\partial(\rho U_i)}{\partial x_i} = 0 \tag{2}$$

Momentum equations

$$\begin{aligned}\frac{\partial(\rho U_i U_j)}{\partial x_j} &= -\frac{\partial P}{\partial x_i} + \frac{\partial}{\partial x_i}[\Gamma(-\frac{2}{3}\frac{\partial U_j}{\partial x_j})] \\ &\quad + \frac{\partial}{\partial x_j}[\Gamma(\frac{\partial U_i}{\partial x_j} + \frac{\partial U_j}{\partial x_i})] \\ &\quad - \frac{2}{3}\frac{\partial(\rho k)}{\partial x_i} + \rho g_i \end{aligned}\tag{3}$$

where U_i is the mean value of the instantaneous velocity u_i given by $U_i + u_i'$, u_i' is the fluctuating velocity, ρ is the density of fluid, $\Gamma = \mu + \mu_t$ is the effective viscosity which is the sum of dynamic viscosity, μ, plus turbulent viscosity, μ_t, k is the turbulent kinetic energy, and g_i is the gravitational constant.

Turbulence effects upon the mean flow are modeled through the eddy viscosity concept, which states that the turbulent stresses are related to the mean strain rate via the turbulent viscosity μ_t. A low Reynolds number k-ϵ model similar to the one proposed in [5] is used to calculate the eddy viscosity, μ_t. The transport equations of k and ϵ are:

$$\frac{\partial(\rho U_i k)}{\partial x_i} = \frac{\partial}{\partial x_i}[(\mu + \frac{\mu_t}{\sigma_k})\frac{\partial k}{\partial x_i}] + P_1 - \rho\epsilon \tag{4}$$

$$\begin{aligned}\frac{\partial(\rho U_i \epsilon)}{\partial x_i} &= \frac{\partial}{\partial x_i}[(\mu + \frac{\mu_t}{\sigma_\epsilon})\frac{\partial \epsilon}{\partial x_i}] + \\ &\quad \frac{\epsilon}{k}(C_1 P_1 - C_2 f_1 \rho\epsilon)\end{aligned}\tag{5}$$

where $P_1 = -\overline{\rho u_i' u_j'}\frac{\partial U_i}{\partial x_j}$, $\mu_t = \frac{C_\mu \rho k^2}{\epsilon}$, $C_\mu = 0.09$, $C_1 = 1.45$, $C_2 = 1.9$, $\sigma_k = 1$, $\sigma_\epsilon = 1.3$, $f_1 = 1 - 0.3\exp(-Re_t^2)$, $Re_t = \frac{\rho k^2}{\mu\epsilon}$, and ϵ is the dissipation rate of turbulent kinetic energy.

3 Equations of particle motion

The motion of a single spherical solid particle in the turbulent flow field is assumed to follow:

$$\frac{du_{pi}}{dt} = \frac{u_i - u_{pi}}{\tau_a} f + g_i \tag{6}$$

$$\frac{dy_i}{dt} = u_{pi} \tag{7}$$

where u_{pi} is velocity of particle, $\tau_a = \rho_p d_p^2/18\mu$ is the aerodynamic response time for the linear Stokes drag, y_i is the trajectory of the particle, and f is a factor accounting for the inertial effect of the drag term. $f = 1$ for linear drag law; for nonlinear drag law, $f = 1 + 0.15Re_p^{0.687}$. This expression tends to give reliable results for values of Re_p up to 1000[6]. $Re_p = \rho d_p|u_i - u_{pi}|/\mu$ is the Reynolds number based on the relative velocities between fluid and particle, d_p is diameter of particle, and ρ_p is density of particle. The density of particle is much denser than that of the fluid such that the Basset force, inertia force of added mass, buoyancy force, and force due to pressure gradients in the flow are negligible. If index notation 1 and 2 are used to represent the horizontal directions, and 3 the vertical direction with positive upward, then

$$\frac{du_{pi}}{dt} = \frac{u_i - u_{pi}}{\tau_a} f - g\delta_{i3} \tag{8}$$

$$\frac{dy_i}{dt} = u_{pi} \tag{9}$$

The initial conditions used are

$$y_i = 0 \quad \text{at} \quad t = 0 \tag{10}$$

$$u_{pi} = u_i(0,0) \quad \text{at} \quad t = 0 \tag{11}$$

4 Modelling of the particle dispersion

The motion of a dispersed particulate phase in the turbulence is determined by the particle-eddy interaction model proposed by Gosman and Ioannides[7]. The interaction between the particle and the eddy for a period of time is the minimum between an estimated particle transit time within the eddy, t_{tr} and an eddy lifetime, t_e. The particle transit time is obtained as the solution of the linearized equation of motion of the particle with the assumption of Stokesian drag and negligible body force. The Lagrangian time scale of the turbulent eddy is obtained from the length and velocity scales of the turbulence, which are extracted from the k-ε turbulence model being employed. Thus,

$$t_{int} = min(t_{tr}, t_e) \tag{12}$$

where

$$t_{tr} = -\tau_a \ln(1.0 - \frac{l_e}{\tau_a |u_i - u_{pi}|}) \tag{13}$$

$$t_e = \frac{l_e}{(2k/3)^{1/2}} \tag{14}$$

The eddy length macroscale, l_e, is defined in terms of the kinetic energy of the turbulence, k and its dissipation rate, ϵ, as

$$l_e = {C_\mu}^{3/4} k^{3/2} / \epsilon \tag{15}$$

In the present study, the fluctuating component of the fluid velocity, u_i', is obtained from a Gaussian distribution of values having a zero mean and a standard deviation, $|u_i'|$ given by

$$|u_i'| = (2k/3)^{1/2} \tag{16}$$

5 Validation of the numerical model for turbulent flow

Detailed experimental measurements of heavy particle dispersion in grid-generated turbulence were made by Snyder and Lumley[4]. They studied the particle motion in a vertical wind tunnel with air flowing upward (i.e., x_3-direction) and the gravity vector opposite to the flow direction. The grid-generated turbulent flow field of Snyder and Lumley[4] is simulated by the k-ϵ model with the RANS equations of the present study. Figure 1 depicts the predicted and experimental turbulence field described in terms of k and ϵ. The predictions compare well with the experiments, with a maximum deviation of less than 5%. Figure 2 shows the predicted energy decay curve along centerline of test section of [4]. The quantity $\overline{u_3^2}$ is assumed to be equal to $\overline{u_2^2}$(i.e., isotropic turbulence) in the present study. Also shown in this figure are the experimental data for the energies of the longitudinal velocity component and the lateral component obtained by Snyder and Lumley[4]. Again, the present predicted results are in good agreement with experimental findings. Hence, it further proves that the simulated turbulent flow field is ready for use later on in the calculation of relative velocity between particle and fluid.

6 Results and discussion

Snyder and Lumley[4] obtained in their experiment the mean square dispersion in the direction perpendicular to the mean flow for four types of spherical particles, -hollow glass

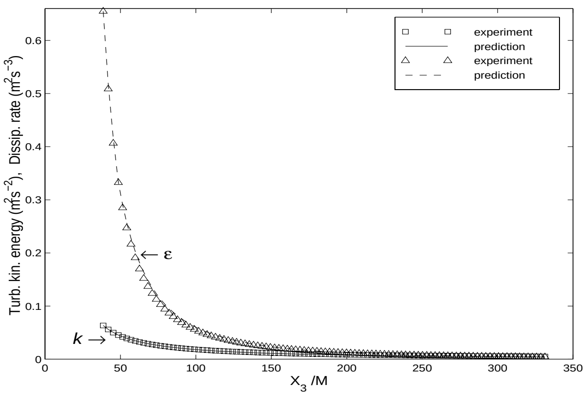

Figure 1: Predictions and experiments of turbulent kinetic energy and dissipation rate (x_3 is the streamwise direction and M=0.0254m is the grid spacing used in [4]).

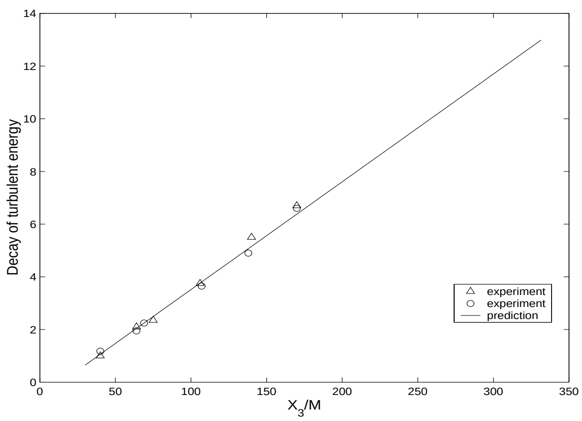

Figure 2: Decay of turbulent energy, $\triangle$, $U^2/\overline{u_3^2} \times 10^{-3}$; $\bigcirc$, $U^2/\overline{u_2^2} \times 10^{-3}$, $U = 6.55m/s$ based on Snyder and Lumley[4].

beads (diameter $d_p = 46.5\mu m$, relaxation time $\tau_a = 1.7ms$, terminal velocity $U_T = 1.67cm/s$), solid glass beads ($d_p = 87.0\mu m$, $\tau_a = 45ms$, $U_T = 44.2cm/s$), corn pollen ($d_p = 87.0\mu m$, $\tau_a = 20ms$, $U_T = 19.8cm/s$), and copper beads ($d_p = 46.5\mu m$, $\tau_a = 49ms$, $U_T = 48.3cm/s$). In simulating their experiment, the particles are released at $x_3/M = 30$, where $M = 0.0254m$ is the grid spacing used in [4]. The calculation of particle dispersion should be started right after the particles pass $x_3/M = 68.4$, which is the location where Snyder and Lumley[4] started performing their measurements. The calculation of the particle dispersion that is free from the effect of initial condition can be achieved only if calculation is performed after the value of $|u_{pi} - u_i|$ has reached its maximum[1]. In order to see if this condition is satisfied or not, the spatial development of the mean square relative velocity between the particle and the local fluid point is performed and the results are presented in Figs. 3 and 4 for nonlinear and linear drag formulations, respectively. The occurrence of the maximum $|u_{pi} - u_i|$ is at the location about $x_3/M = 35 - 37$ for nonlinear drag, and $x_3/M = 37 - 76$ for linear drag, depending on the values of τ_a and U_T. For the nonlinear drag calculation, the occurrence of the maximum value of $|u_{pi} - u_i|$ is well ahead of the location $x_3/M = 68.4$, where the particle dispersion measurement is taken. For the linear drag calculation, however, the occurrence of the maximum value of $|u_{pi} - u_i|$ is at a location right after $x_3/M = 68.4$ for heavy particles(i.e., solid glass and copper), while for light particles(i.e., hollow glass and corn), it is still well ahead the location $x_3/M = 68.4$. Hence, better predictions of particle dispersion obtained with the nonlinear drag formulation, especially for heavy particles, should be expected.

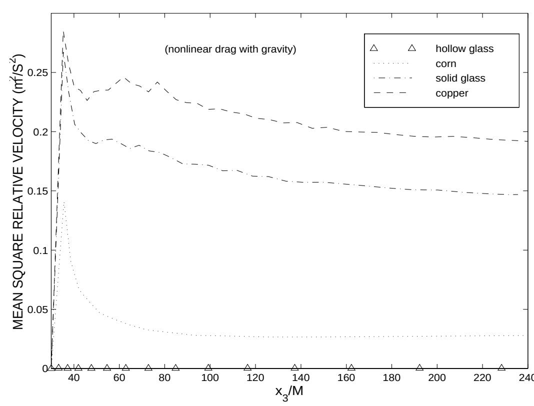

Figure 3: Spatial development of the mean square relative velocity of the particle, $\overline{u_{i,rel}^2}$, for nonlinear drag with gravitational effect.

Figures 3 and 4 illustrate that, at zero time, $\overline{u_{i,rel}^2}$ is zero because of the imposed initial con-

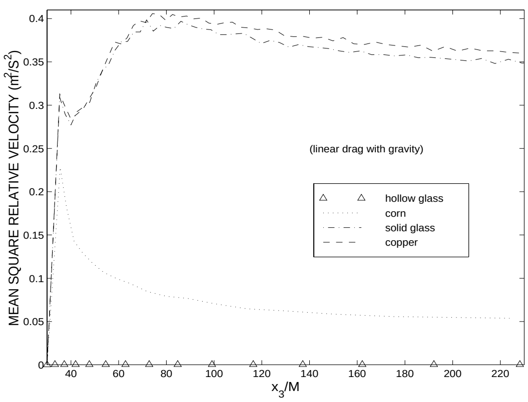

Figure 4: Spatial development of the mean square relative velocity of the particle, $\overline{u_{i,rel}^2}$, for linear drag with gravitational effect.

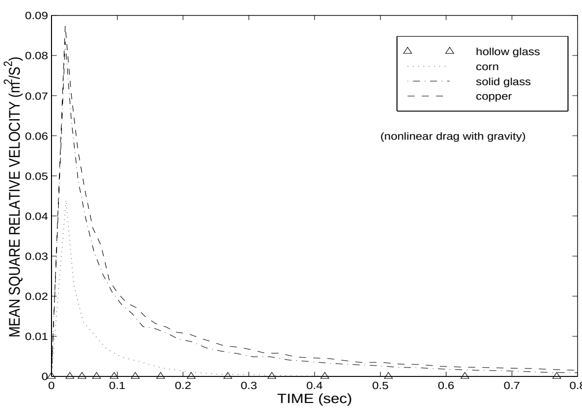

Figure 5: Mean square relative velocity of the particle in the direction normal to the gravity, $\overline{u_{1,rel}^2}$, for nonlinear drag with gravitational effect.

dition. $\overline{u_{i,rel}^2}$ goes to a maximum and then decays to a constant asymptotically. The values of the maximum and the constant depend on different types of particles. Both of them are larger for particles with higher relaxation time(τ_a). It is also noted from Figs. 3 and 4 that there are differences in spatial development of $\overline{u_{i,rel}^2}$ between nonlinear and linear drag formulations for each type of particle, with the possible exception of the hollow glass. These differences in maximum values and asymptotic constants can be attributed to the fact that particles settle at a larger velocity in linear drag formulation than that in nonlinear drag formulation[8]. It is noted that Figs. 3, and 4 present more than one local maximum value of $|u_{pi} - u_i|$ for heavy particles, these can be attributed to the fact that the maximum value of $|u_{p1} - u_1|$(or $|u_{p2} - u_2|$) and $|u_{p3} - u_3|$ occur at different locations. And these are illustrated in Figs. 5 and 6, and Figs. 7 and 8 for nonlinear, and linear drag, respectively. When comparing these figures, it is found that, for both nonlinear and linear drag formulations, $\overline{u_{1,rel}^2}$ reaches its maximum well ahead of $\overline{u_{3,rel}^2}$ does. This phenomenon holds for all types of particles with the exception of hollow glass. It is also noted that $\overline{u_{3,rel}^2}$ approaches an invariant value as time develops. But this invariant value is different between nonlinear and linear drag formulations. With a larger values of $\overline{u_{3,rel}^2}$ for linear drag formulation as expected[8].

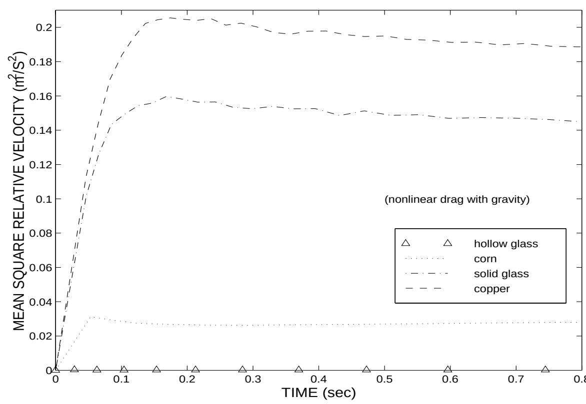

Figure 6: Mean square relative velocity of the particle in the gravity direction, $\overline{u_{3,rel}^2}$, for nonlinear drag with gravitational effect.

7 Concluding Remarks

Mean square relative velocity between particle and fluid in a grid-generated turbulent flow field is studied numerically. Simulation results with linear drag formulation using heavy particles show that maximum value of mean square relative velocity between particle and fluid has not been reached at the location

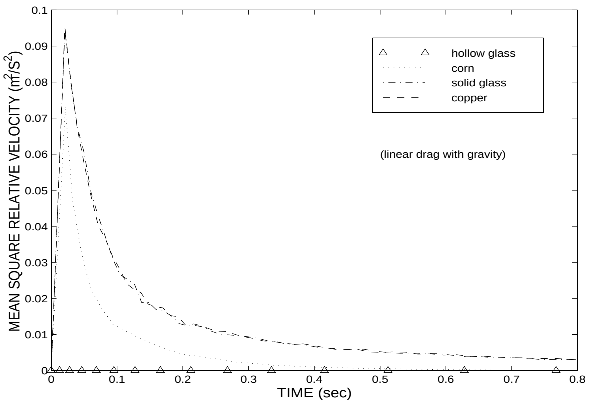

Figure 7: Mean square relative velocity of the particle in the direction normal to the gravity, $\overline{u^2_{1,rel}}$, for linear drag with gravitational effect.

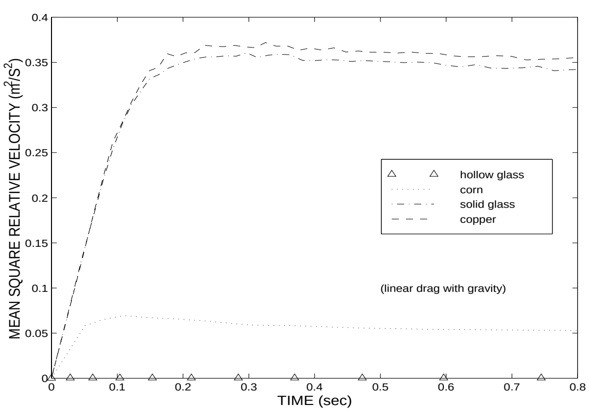

Figure 8: Mean square relative velocity of the particle in the gravity direction, $\overline{u^2_{3,rel}}$, for linear drag with gravitational effect.

where particle mean square displacement measurement has been taken in Snyder and Lumley's experiment[4]. On the other hand, results of nonlinear drag formulation show that the mean square relative velocity reaches its maximum well before the position where the particle mean square displacement measurement was taken as reported in [4]. Numerical results also show that the mean square relative velocity components in the gravity direction and in the direction normal to the gravity reach the maximum values at different times.

References:

[1] Riley, J. J., and Patterson, G. S., "Diffusion experiments with numerical integrated isotropic turbulence," *Physics of Fluids*, 17, 1974, pp. 292-297.

[2] Yeh, F., and Lei, U., "On the motion of small particles in a homogeneous isotropic turbulent flow," *Physics of Fluids A*, Vol. 3, 1991, pp. 2571-2586.

[3] Elghobashi, S., and Truesdell, G. C., "Direct simulation of particle dispersion in a decaying isotropic turbulence," *Journal of Fluid Mechanics*, Vol. 242, 1992, pp. 655-700.

[4] Snyder, W. H., and Lumley, J. L., "Some measurements of particle velocity autocorrelation functions in a turbulent flow," *Journal of Fluid Mechanics*, Vol. 48, 1971, pp. 41-71.

[5] Lopes, A. M. G., Sousa, A. C. M., and Viegas, D. X., "Numerical simulation of turbulent flow and fire propagation in complex topography," *Numerical Heat Transfer*, Part A, 27, 1995, pp. 229-253.

[6] Clift, R., Grace, J. R., and Weber, M. E., *Bubbles, drops and particles*, Academic Press, New York, 1978.

[7] Gosman, A. D., and Ioannides, E.,"Aspects of computer simulation of liquid-fuelled combustors," *paper AIAA-81-0323*, AIAA 19th Aerospace Sciences Meeting, 1981, St Louis, Missouri.

[8] Sin, V. K., "Studies of the Settling Velocity of Heavy Particles in Homogeneous Isotropic Turbulence and Random Flow Field," *Proceedings of the eighth International Conference on Enhancement and Promotion of Computational Methods in Engineering Science (EPMESC'VIII*, July 25-28, 2001, Shanghai, China, CR-ROM.